
Capacity of Multi-Antenna Array Systems

Chen-Nee Chuah

supervised by
Professor Joseph Kahn and Professor David Tse

Department of Electrical Engineering and Computer Sciences
University of California
Berkeley, CA 94720

January 25, 2000

Abstract:

This work is inspired by the large capacity increase that may be achieved by using multi-element antenna arrays (MEA) at both transmitting and receiving sites. We present a numerical study of the information-theoretic capacity of indoor wireless systems that employ MEAs, based on realistic ray-tracing modeling of propagation in an office building. The Shannon capacity for multi-antenna systems assuming that the transmitter knows the channel (C_n) is computed, and is compared to the mutual information achieved with equal power allocation when the transmitter does not know the channel (MI_n). Results show that for a fixed average received SNR, the gap between C_n and MI_n grows as the number of antennas is increased. We also investigate the effect of the received SNR on C_n and MI_n . We derive expressions for the asymptotic growth of capacity as the number of antennas grows large and compare these asymptotic results with the capacities computed using simulated channel responses. The results reported in this paper serve as a preliminary exploration of MEA systems, and we anticipate obtaining different capacity estimates for different environments or when actual measurements are made.

This work was supported by the University of California MICRO Program.

CONTENTS

- I. Introduction. 1
- II. Channel Model 2
- III. Information-Theoretic Results 4
 - A. Capacity Without Channel Knowledge at the Transmitter 4
 - B. Capacity With Perfect Channel Knowledge at the Transmitter 4
 - C. Asymptotic Behavior of Capacity 6
 - 1. With Perfect Channel Knowledge at the Transmitter 7
 - 2. Without Channel Knowledge at the Transmitter 8
- IV. Numerical Studies Using WiSE. 9
 - A. WiSE System Model 9
 - 1. Channel Outage 10
 - 2. Received SNR 11
 - B. Simulation Results and Discussions 11
 - 1. Capacity Improvement due to Water Filling 12
 - 2. Asymptotic Behavior of Capacities 14
- V. Conclusions 15
- VI. Acknowledgments 17
- VII. References 18
- VIII. Tables 19
- IX. Figures. 20
- Appendix A: Capacity for Channels with Frequency-Selective Fading. 29

I. Introduction

In order to meet the competitive demand for higher and higher bit rates in wireless local-area networks (LANs), researchers have explored the utilization of multiple-element arrays (MEAs) at both transmitting and receiving sites. Space diversity has long been known to improve reception of signals for wireless systems. Numerous studies have considered using multiple receivers to combat multipath fading of the desired signal, or to suppress interfering signals [1], [2]. Using diversity at both transmitters and receivers promises a huge capacity gain because of the additional spatial degrees of freedom it affords. One fundamental question arises: how many bits per second per Hertz can one transmit from a transmitting MEA to a receiving MEA given a specific propagation environment?

Foschini and Gans reported information-theoretic MEA capacities in [3], [4] for a narrowband Rayleigh fading environment, with i. i. d. channel responses between each antenna pair. They assume that the transmitter does not know the channel, and equal number of antennas, n , are used at both transmitter and receiver. Foschini and Gans showed that for large n , the capacity increases linearly with n in this case. Our work **seeks to determine** whether the capacity will further increase if the transmitter knows the channel, **and if so**, is the increase significant enough to justify the **additional complexity** required in signal processing and feedback from the receiver to the transmitter. In addition, we also investigate whether the linear capacity growth found in [4] can be retained in a more realistic propagation environment, in which the transmitted and received signals are correlated or when there is a dominant line-of-sight (LOS) signal.

We only consider a point-to-point link with additive Gaussian noise between the transmitter and the receiver, assuming there is no co-channel (multi-user) interference. We use the WiSE [5] simulation tool to model the indoor channel from a base station to receivers located in different rooms of an office building. A 5.2-GHz carrier is launched from transmitting antennas, and the amplitudes, delays and phase angles of rays impinging on the receiving antennas are recorded. Similar studies have been reported by Foschini and Valenzuela for MEA systems operating at 5.2 GHz [6].

The remainder of this paper is organized as follows. In Section II, we model the channel as a multiple-input-multiple-output (MIMO) system with flat frequency response. Using this mathematical

model in Section III, we present information-theoretic results for the capacity of MEA systems and analyze its asymptotic behavior as the number of antennas grows large. In Section IV, we present capacity estimates for the simulated channels and discuss the discrepancies between these results and the asymptotic capacities predicted by theory. We briefly describe how WiSE is used to represent the indoor propagation environment that our numerical study is based on. We also include details about placements of transmitting and receiving MEA, arrangement of antennas in an array, and basic assumptions for the antenna elements. Then conclusions are presented in Section V.

II. Channel Model

The following notation will be used throughout the paper: $'$ for vector transpose, † for transpose conjugate, I_n for the $n \times n$ identity matrix, $E[\cdot]$ for expectation, $*$ for convolution, and underline for vectors.

We consider a single-user, point-to-point communication channel with n transmitting antennas and n receiving antennas. The transmitted signal is $\underline{X}(t) = [x_1(t), x_2(t), \dots, x_T(t)]'$, an $n \times 1$ vector whose j th component represents the signal transmitted by the j th antenna. Similarly, the received signal and received noise are represented by $n \times 1$ vectors, $\underline{Y}(t)$ and $\underline{Z}(t)$, respectively, where $y_i(t)$ and $z_i(t)$ represent the signal and noise received at the i th antenna. The complex baseband impulse response between antenna i and antenna j is represented by $h_{ij}(t)$, for $i = 1, 2, \dots, n$ and $j = 1, 2, \dots, n$. Assuming that the channel is linear and time-invariant, the transmitted and received vectors are related by:

$$\underline{Y}(t) = h(t) * \underline{X}(t) + \underline{Z}(t) \quad (1)$$

We assume the communication bandwidth, W , that we consider throughout this **report** is narrow enough that the channel frequency characteristic can be treated as flat over frequency. For this to be a reasonable approximation, the communication bandwidth must be much less than the coherent bandwidth. We have determined from WiSE that, for our channels, the maximum delay spread¹ is 24 ns. The coherence bandwidth is approximately the reciprocal of the multipath delay spread, which is 41.7 MHz. Therefore the frequency response can indeed be considered flat for a communication

¹. Delay spread here refers to the difference, maximum delay - minimum delay, of strong rays that arrive at the receiver with power above a chosen threshold.

bandwidth much less than 40 MHz, or a symbol rate much less than 80 Mbaud/s, assuming zero excess bandwidth.

For the remaining analysis and discussions, we use the discrete-time equivalent model and (1) can be simplified to:

$$\underline{Y} = H\underline{X} + \underline{Z} \quad (2)$$

where $\underline{X}, \underline{Y}, \underline{Z} \in C^n$ and $H \in C^{n \times n}$ whose entry H_{ij} , which is the discrete time sample of $h_{ij}(t)$, represents the fading path gain from antenna j to antenna i .

We further assume that:

- The symbol duration is short compared to the coherence time¹ of the channel. Hence, the channel response H is fixed throughout the time scale that we consider.
- The total radiated average power (sum over all transmitting antennas) is P_{tot} , regardless of the number of transmitting antennas n .
- The noise vector, \underline{Z} , is an additive white complex Gaussian random vector, which means its components, Z_i for $i = 1, 2, \dots, n$, are i. i. d. circularly symmetric complex Gaussian random variables with variance $E[|Z_i|^2] = N_0 W$ where W is the signal bandwidth.

We consider the following two cases:

1. H is known only to the receiver but not the transmitter. Power is distributed equally over all transmitting antennas in this case.
2. H is known at the transmitter and receiver, so that power can be allocated appropriately to maximize the achievable rate over the channel.

In this work, we treat H as quasi-static. Since H is fixed for the whole duration of communication, capacity can be computed for each realization of H without time averaging. On the other hand, H changes if the receiver is moved from one place to the other, i.e. H varies over a much larger time scale than a specific communication session when the receiver remains fixed on the same location. Therefore, the associated capacity and mutual information for each specific realization of H can be viewed as random variables that depend on the location of transmitting and receiving MEA.

¹. Coherence time of the channel refers to the duration for which the channel response remains constant.

III. Information-Theoretic Results

In this section, we state the generalized formula for capacity for different cases. The transmitting MEA sends the signal vector \underline{X} , which consists of symbols chosen from some alphabet set. The reception is subject to additive white Gaussian noise. Channel capacity is defined as the highest rate at which information can be sent with arbitrarily low probability of error (Chapter 8, [7]).

For the case with one antenna, $n = 1$, the Shannon capacity is:

$$C(P_{\text{tot}}, H) = \log_2 \left(1 + \frac{P_{\text{tot}} |H|^2}{N_0 W} \right) \text{ bps/Hz.} \quad (3)$$

In the high-SNR regime, each 3-dB increase of $P_{\text{tot}}/N_0 W$ yields a capacity increase of 1 bps/Hz.

A. Capacity Without Channel Knowledge at the Transmitter

Here, we assume that the transmitter does not know the channel, and equal power is radiated from each transmitting antenna. The mutual information in this case is denoted by MI_n (when n transmitting and n receiving antennas are used), and has been derived in [3] as:

$$MI_n(P_{\text{tot}}, H) = \log_2 \det \left[I_n + \left(\frac{P_{\text{tot}}}{n N_0 W} \right) \cdot H H^\dagger \right] \text{ bps/Hz,} \quad (4)$$

where H is an $n \times n$ matrix that represents the channel as in (2).

B. Capacity With Perfect Channel Knowledge at the Transmitter

In this section, we derive the capacity for MIMO channel assuming the transmitter has perfect knowledge about the channel. This assumption is reasonable if the channel is changing very slowly, so that it can be tracked by the transmitter through feedback from the receiver. With this knowledge of the channel, total transmit power can be allocated in the most efficient way over the different transmitting antennas to achieve the highest possible bit rate, and we refer to this as the *optimal power allocation*. Based on the model in Section II and definitions in [7], the MEA capacity with optimal power allocation, C_n , can be derived as follows:

$$C_n(P_{\text{tot}}, H) = \max_Q \log_2 \det \left[I_n + \frac{H Q H^\dagger}{N_0 W} \right] \text{ bps/Hz,} \quad (5)$$

subject to the average power constraints:

$$\text{tr}(Q) = \sum_{i=1}^n E[\underline{X}_i^2] \leq P_{\text{tot}}, \quad (6)$$

where Q is the $n \times n$ covariance matrix of \underline{X} , $Q = E[\underline{X}\underline{X}^\dagger]$ and P_{tot} is the total average transmit power.

By singular value decomposition, $H = UDV^\dagger$, where U and V are unitary matrices. $D \in R^{n \times n}$ is diagonal and has non-negative entries, which are the square roots of the eigenvalues of HH^\dagger . We can rewrite (2) as

$$\underline{Y} = UDV^\dagger \underline{X} + \underline{Z}. \quad (7a)$$

If we let $\tilde{\underline{Y}} = U^\dagger \underline{Y}$, $\tilde{\underline{X}} = V^\dagger \underline{X}$, and $\tilde{\underline{Z}} = U^\dagger \underline{Z}$, (7a) becomes

$$\tilde{\underline{Y}} = D\tilde{\underline{X}} + \tilde{\underline{Z}}. \quad (7b)$$

Since U^\dagger is unitary, $\tilde{\underline{Z}}$ is just a rotation of \underline{Z} in n -dimensional space, $\tilde{\underline{Z}}$ therefore has the same distribution as \underline{Z} , i.e. $\tilde{\underline{Z}}$ is also a white complex Gaussian random vector.

We define $\tilde{Q} = E[\tilde{\underline{X}}\tilde{\underline{X}}^\dagger]$, which is related to Q by:

$$\tilde{Q} = V^\dagger Q V. \quad (7c)$$

Since unitary operators preserve the inner product, $\text{tr}(\tilde{Q}) = \text{tr}(Q)$. Hence, (5) and (6) can be simplified to:

$$C_n(P_{\text{tot}}, H) = \max_{\tilde{Q}} \log_2 \det \left[I_n + \frac{D^2 \tilde{Q}}{N_0 W} \right], \quad (8a)$$

and

$$\text{tr}(\tilde{Q}) \leq P_{\text{tot}}. \quad (8b)$$

To maximize the mutual information to achieve capacity, we need to choose $\tilde{\underline{X}}_i$ to be independent complex Gaussian ([8]), i.e. \tilde{Q} should be diagonal. The diagonal entries \tilde{Q}_{ii} (the variances of $\tilde{\underline{X}}_i$) are chosen such that the average power constraint (8b) is satisfied. The total capacity can be expressed as:

$$C_n(P_{\text{tot}}, H) = \max_{\tilde{Q}_{ii}} \sum_{i=1}^n \log_2 \left[1 + \frac{\lambda_i \tilde{Q}_{ii}}{N_0 W} \right], \quad (9)$$

subject to the same power constraint (8b). This optimization problem can be solved by using Lagrange multipliers, which gives us the following optimum solutions:

$$\tilde{Q}_{ii}^* = \left(\mu - \frac{N_0 W}{\lambda_i} \right)^+, \quad (10a)$$

for $i = 1, 2, \dots, n$ where μ satisfies

$$\sum_i \left(\mu - \frac{1}{\lambda_i} \right)^+ = P_{\text{tot}}. \quad (10b)$$

Therefore,

$$C_n(P_{\text{tot}}, H) = \sum_{i=1}^n \log_2 (\lambda_i \mu)^+. \quad (11)$$

The optimal solution, (10a) and (10b), is analogous to the water-filling solutions for parallel Gaussian channels discussed by Cover and Thomas in [7]. Intuitively, the above equation suggests that the original channel can virtually be decomposed into n parallel independent sub-channels, and we allot power to the channels with higher SNRs (smaller $N_0 W / \lambda_i$). Here, μ is the “water level” that marks the height of the power that is poured into the “water vessel” formed by the function $N_0 W / \lambda_i$, $i = 1, 2, \dots, n$. When the available power P_{tot} is increased, some of the power will be allocated to the noisier channels. Each of these sub-channels contributes to the total capacity through $\log_2 (\lambda_i \mu)^+$. If

$$\lambda_i \mu \gg 1, \quad (12)$$

we say that this sub-channel provides an effective mode of transmission and the corresponding λ_i is called a *strong eigenmode*. If all the eigenvalues are much larger than $1/\mu$, the capacity is a sum of n terms of a similar magnitude.

C. Asymptotic Behavior of Capacity

We investigate the growth of capacity of MEA system as the number of antennas grows large for two cases: (a) when the transmitter knows the channel and (b) when it does not. The capacity, MI_n and

C_n are random variables that depend on the specific realization of H . The channel is described by equation (2), and we assume that \underline{Z} is complex, zero mean white Gaussian noise vector with variance N_0W , and H has i. i. d. complex entries with variance $E|H_{ij} - E(H_{ij})|^2 = \nu^2$. All the assumptions in Section II hold. For simplicity, when n antennas are used, we denote $MI_n(P_{\text{tot}}, H)$ and $C_n(P_{\text{tot}}, H)$ as MI_n and C_n respectively.

1. With Perfect Channel Knowledge at the Transmitter

For a given H , the capacity is given by the water-filling solution (9):

$$C_n(P_{\text{tot}}, H) = \sum_{i=1}^n (\log_2(\mu\lambda_i))^+ \quad (13a)$$

where μ satisfies

$$\sum_i \left(\mu - \frac{1}{\lambda_i}\right)^+ = P_{\text{tot}} \quad (13b)$$

and λ_i are the eigenvalues of HH^\dagger , which are random variables that depend on the realization of H . For each n , let F_n be the empirical distribution of λ_i , i.e., the fraction of λ_i less than or equal to λ for the case with n antennas:

$$F_n(\lambda) = \frac{1}{n} |\{i: (\lambda_i \leq \lambda)\}|.$$

Note that the capacity depends on H only through the empirical distribution of λ_i , $F_n(\lambda)$. The asymptotic properties of the random variable C_n depends on how the distribution F_n behaves as n approaches infinity. The following theorem is the result of the work by Marcenko, Yin, Silverstein et al in [9]-[11].

Theorem 1. Define $G_n(\lambda) := F_n(n\lambda)$. Then, almost surely, G_n converges to a nonrandom distribution G^* , which has a density given by:

$$g^*(\lambda) = \begin{cases} \frac{1}{\pi} \sqrt{\frac{1}{\lambda} - \frac{1}{4}} & 0 \leq \lambda \leq 4 \\ 0 & \text{otherwise.} \end{cases}$$

The scaling by n in the definition of F_n means that the λ_i are growing as order n . After rescaling, the distribution converges to a deterministic limiting distribution, i.e. for large n , the empirical distribution of the singular values looks similar for almost all realization of H . Using this theorem, we get the following result:

Proposition 1.1. Let $\alpha = \frac{v^2 P_{\text{tot}}}{N_0 W}$. Almost surely,

$$\frac{C_n(P_{\text{tot}}, H)}{n} \rightarrow C^*(\alpha),$$

where

$$C^*(\alpha) = \int_0^4 (\log_2(\mu\lambda))^+ \cdot g^*(\lambda) d\lambda \quad (14a)$$

and μ satisfies

$$\int_0^4 \left(\mu - \frac{1}{\lambda}\right)^+ \cdot g^*(\lambda) d\lambda = \alpha. \quad (14b)$$

This indicates that C_n scales like nC^* .

2. Without Channel Knowledge at the Transmitter

Let us now consider the case when the transmitter does not have any information about the channel, and always allocates an equal power P_{tot}/n to each of the transmitting antennas. The mutual information under equal power allocation is

$$MI_n = \sum_{i=1}^n \log_2 \left(1 + \frac{P_{\text{tot}}}{nN_0W} \lambda_i \right), \quad (15)$$

where $\{\lambda_i\}$ are the eigenvalues of HH^\dagger . Using Theorem 1, we can prove the following proposition.

Proposition 1.2. Again let $\alpha = \frac{v^2 P_{\text{tot}}}{N_0 W}$. With almost sure convergence,

$$\frac{MI_n(P_{\text{tot}}, H)}{n} \rightarrow MI^*(\alpha),$$

where

$$MI^*(\alpha) = \int_0^4 (\log_2(1 + \alpha\lambda))^+ \cdot g^*(\lambda) d\lambda. \quad (16)$$

With the above two propositions, we get

$$\frac{C_n}{MI_n} \rightarrow \frac{C^*}{MI^*} \text{ almost surely.}$$

The above ratio quantifies the performance gain achieved asymptotically by water-filling, and depends only on α . Using L'Hopital's rule, it can be shown that at low SNR,

$$\lim_{P_{\text{tot}} \rightarrow 0} \frac{C^*}{MI^*} = 4,$$

while at high SNR,

$$\lim_{P_{\text{tot}} \rightarrow \infty} \frac{C^*}{MI^*} = 1.$$

In the next section, we estimate the average capacities \overline{C}_n and \overline{MI}_n of simulated channel responses and study how they grow at large n . The simulation results are then compared to the asymptotic results nC^* and nMI^* derived above.

IV. Numerical Studies Using WiSE

A. WiSE System Model

We use the experimentally based Wireless System Engineering (WiSE) ray tracing simulator to generate realistic realizations of the channel matrix H for indoor wireless propagation. C_n and MI_n are then computed for each realization of H . WiSE has been developed by Steve Fortune et al at Bell Laboratories [5] to model radio propagation in buildings. The predicted baseband channel impulse response is of the form:

$$h(t) = \sum_{k=0}^M \beta_k \cdot e^{i\theta_k} \cdot \delta(t - \tau_k), \quad (17)$$

where β_k is the real positive gain, θ_k the associated phase shift, and τ_k the propagation delay of the k th ray. M is the total number of rays and $\delta(t)$ is the unit impulse function. We can compute the frequency response as:

$$H(f) = \sum_{k=0}^M \beta_k \cdot e^{i\theta_k} \cdot e^{i2\pi f\tau_k}, \quad (18)$$

As long as the communication bandwidth W is narrower than the coherence bandwidth, $H(f)$ can be considered constant over the band of interest. For our analysis, we evaluated $H(f)$ at the carrier frequency, f_c .

In our work, we model the first floor of a two-floor office building at Crawford Hill, New Jersey (see Fig. 1) in WiSE. We consider the case of multiple omnidirectional transmitting and receiving antennas, with a 5.2-GHz carrier frequency. For all the simulations, we place the transmitting MEA on the first floor ceiling near the middle of the office building (see Fig. 1). Antennas are arranged in square grids within horizontal planes at both the transmitting and receiving sites. The separation between antenna elements is the same at both the transmitting and receiving MEAs. The antenna spacing is denoted as d and we consider $d = 0.5\lambda$ (2.9 cm). The location of the transmitter is fixed. Receiving antenna-arrays are placed with random rotations on the horizontal plane at 1000 randomly chosen positions in each of three rooms: L117 (closest to the transmitter), L147 (at intermediate distance) and L175 (furthest from the transmitter).

H varies for different receiver locations. When we take expectation with respect to different realizations of H , we mean taking the ensemble average over the 1000 sample receiver locations. The capacities with and without water filling, C_n and MI_n , are computed for different n . Since the channel changes as the receiver is moved around, the capacity is treated as a random variable. The values of C_n and MI_n vary for different receive locations. The results will be presented in terms of complementary cumulative distribution functions (CCDFs). The averages, \bar{C}_n and \bar{MI}_n are then computed.

1. Channel Outage

As mentioned before, capacity is dependent on the channel realization and hence might change considerably when the receiver is moved from one place to another. The communication is considered

successful only if the capacity is above a certain threshold. When this is not met, we say that a channel outage has occurred. Outage is a probabilistic event and we are interested in its tail distribution. The figures of merit that are of greatest interest are the values of C_n and MI_n that can be attained with probability $1 - \varepsilon$, denoted as C_n^ε and MI_n^ε . For example, $P(C_n < C_n^\varepsilon) = \varepsilon$. Here we consider $\varepsilon = 0.05$ and call this 5 % channel outage. From the CCDFs that we obtain from WiSE, we determine the capacities at 5 % outage probability, $C_n^{0.05}$ and $MI_n^{0.05}$.

2. Received SNR

We assume the fading path gains, H_{ij} , for $i, j = 1, 2, \dots, n$, are identically distributed with the same variance v^2 . We assume that v^2 is the same for all fading gain H_{ij} for the receiving antennas that are co-located in a specific office room. However, v^2 varies when the receiving MEAs are moved into another office room, for example, v^2 is different between room L117 and L147. Within each room, we estimate $v^2 = E[|H_{ij} - E[H_{ij}]|^2]$, from the channel response H generated using WiSE by averaging over 1000 channel realizations, and over all possible antenna pairs, j to i .

The average received SNR is defined to be

$$\rho = \frac{P_{\text{tot}} \cdot v^2}{N_0 W}, \quad (19)$$

where v^2 is estimated as explained above.

We assume that ρ should be high enough for low-error-rate communication. The appropriate range is 18-22 dB, due to the practical constraints on A/D converters that are available with current technology. For all our simulations, we assume W to be 10 MHz, and N_0 to be -170 dBm/Hz¹, giving a total noise variance $N_0 W$ of -100.8 dBm. P_{tot} is a parameter that we can vary in our experiments in order to vary the received SNR ρ .

B. Simulation Results and Discussions

The larger the separation between the transmitter and the receiver, the smaller the values of achievable capacities C_n and MI_n . Fig. 2 illustrates this phenomenon. The three pairs of curves are the CCDFs of C_n and MI_n in each of the three office rooms for the case when $n = 4$ and the antenna ele-

¹. Typical two sided power spectral density of thermal noise at 300 K (room temperature) for a receiver that is modeled as a 50 ohm resistance is -170.8 dBm/Hz.

ments are separated by $d = \lambda/2$. We fix the transmit power P_{tot} to be 20 dBm, so that $P_{\text{tot}}/N_0 = 120.8$ dB for all three office rooms. The average received SNR, ρ , depends on v^2 , which is different for each office room. From our empirical data, $\rho = 17$ dB when receivers are placed in the furthest room L175, $\rho = 38$ dB for L147 and $\rho = 55.7$ dB for L117. At 5 % outage, $MI_n^{0.05}$ is 60.7 bps/Hz in L117, 18.9 bps/Hz in L147 and 4.6 bps/Hz in L175. For $n = 4$, there are 4 distinct eigenvalues (λ_i) for HH^\dagger . The smaller the separation between the transmitter and receiver, the more strong eigenmodes exists for effective communication, i.e. the larger the fraction of λ_i that satisfy the condition $\frac{P_{\text{tot}}\lambda_i}{N_0W} \gg 1$. Similarly, when optimal power allocation is employed when the separation is smaller, the higher the proportion of the λ_i that satisfy condition (12). Therefore there are more strong sub-channels that contribute to the total capacity in room L117 compared to other rooms. $C_n^{0.05}$ is 60.7 bps/Hz in L117, followed by 19.0 bps/Hz in L147 and 6.3 bps/Hz in L175. With a 10-MHz bandwidth, one can expect capacities in the range of 607 Mbps in L117. Such huge capacities might be too high to be fully exploited in a practical implementation with current technology. Nevertheless, the information-theoretic capacity serves as the ultimate limit for the achievable bit rate.

1. Capacity Improvement due to Water Filling

The advantage of having channel knowledge at the transmitter so that water filling can be employed is illustrated in Fig. 2 by the horizontal gap between the CCDFs of MI_n (solid curves) and C_n . The gain in capacity is more apparent in L175 where there are fewer strong eigenmodes for effective transmission, which explains the wider gap between the solid and dashed curve for L175 compared to the gap for L147 or L117. When all λ_i are equally strong eigenmodes, equal power allocation does as well as the water-filling solutions, resulting in little difference between MI_n and C_n (as in L117). On the other hand, in L175 where only a few λ_i are strong eigenmodes, water filling solution allows us to pour more power into the strong sub-channels. Therefore the strong sub-channels will contribute more to the total capacity C_n . If we allocate power equally over all antennas, some power will be wasted in the weak sub-channels. Therefore, the improvement of C_n over MI_n is more significant in this case. The ratio of improvement at 5 % outage probability $C_n^{0.05}/MI_n^{0.05}$, depends on the SNR level, number of antennas n , and location of the receivers. For example, with $\rho = 38$ dB and $n = 4$, $C_n^{0.05}/MI_n^{0.05} = 1.7, 1.1$ and 1.0 for L175, L147, and L117, respectively.

The difference between C_n and MI_n is dependent on the distribution of λ_i , the average received SNR, ρ , as well as the number of antennas n . To separate the effect that the distribution of λ_i might have, we only consider one office room, L147, in the remaining simulation results and discuss the effect of ρ and n on C_n , MI_n , $C_n^{0.05}$, $MI_n^{0.05}$, and $C_n^{0.05}/MI_n^{0.05}$.

The CCDFs for MI_n and C_n in room L147 are plotted for different antenna array sizes: $n = 1, 4, 9, 16, 25$ and 36 at $\rho = 38$ dB in Fig. 3. The rightward shift of the curves shows that the capacity increases with the number of antennas, n , because space diversity provides additional spatial degrees of freedom for transmission. At 5 % outage, using a single antenna yields $MI_1^{0.05} = 8.63$ bps/Hz while MEA system achieves value up to 19 bps/Hz when $n = 4$ and 33.8 bps/Hz when $n = 9$. Note how the gap between C_n and MI_n (dashed and solid lines, respectively) grows with the array size. $MI_n^{0.05} = 8.63$ bps/Hz when $n = 1$, while $C_n^{0.05} = 8.86$ bps/Hz. This improvement is negligible. However for a system with $n = 4$, the difference between $C_n^{0.05}$ and $MI_n^{0.05}$ is about 1 bps/Hz, which is more than a 5 % improvement. The difference between $C_n^{0.05}$ and $MI_n^{0.05}$ keeps increasing as the number of antennas increases, and reaches 11.32 % for the case $n = 36$. Table 1 summarizes the improvement in capacity when water filling is employed as compared to the case of using equal power allocation at the transmitter. The gain is computed for 5 % outage probability.

In Fig. 4(a), $C_n^{0.05}$ and $MI_n^{0.05}$ are shown by dashed and solid lines, respectively for receivers in L147 at various values of SNR ρ . When ρ is small, there are few strong eigenmodes. Knowing the channel allows us to allocate power more efficiently to stronger subchannels and therefore achieve higher capacity as compared to equal power distribution over all subchannels. As ρ increases, the difference between C_n and MI_n decreases.

The corresponding water-filling gain, $C_n^{0.05}/MI_n^{0.05}$ is plotted in Fig. 5(a). For $n = 4$, the ratio decreases from 3 at $\rho = -10$ dB to 1 at $\rho = 50$ dB. We observe that we need lower average received SNR to achieve the same water-filling gain when the number of antennas increases. This is surprising because the asymptotic results from Section III-C predicts that C_n and MI_n will scale as nC^* and nMI^* respectively. Therefore, one would expect that the ratio will converge to a constant as shown in Section III-C, but this is not the case in Fig. 5(a). To investigate this further, $\overline{C_n}/\overline{MI_n}$ is plotted in Fig. 5(b). At low received SNR, the three solid curves (for $n = 4, 9$ and 16) are closer to one another in Fig.

5(b) compared to the corresponding curves in Fig. 5(a). We conjecture that this is because the rate of convergence for $C_n^{0.05}$ and $MI_n^{0.05}$ (at 5 % outage probability) to the asymptotic value is lower than the rate of convergence for \bar{C}_n and \bar{MI}_n

2. Asymptotic Behavior of Capacities

We also study the behavior of C_n and MI_n as n grows large using channel matrices generated using WiSE. As shown in Fig. 3, the rightward shifts of CCDFs for MI_n and C_n as n increases indicates the capacity gain achieved by using antenna arrays. The theory of Section III-C predicts that as n grows large, the mutual information and capacity of the MIMO channel will scale like nMI^* and nC^* , respectively. Here, we estimate the variance v^2 from the simulated channels to compute nMI^* and nC^* . We note that the asymptotic results of Section III-C, nMI^* and nC^* , assumes i. i. d. channel responses, while the channels used to estimate \bar{MI}_n and \bar{C}_n are subject to correlation between the entries of H .

The average capacity \bar{C}_n increases when the antenna separation d is increased. The \bar{C}_n computed from simulated channels are plotted in Fig. 6(a) as a function of n for different $d = 0.5\lambda$, 1λ and 5λ for high average received SNR, $\rho = 40$ dB. When the antenna spacing is equal to 0.5λ , there is a huge gap between the \bar{C}_n and the nC^* predicted from the asymptotic theory of Section III-C. \bar{C}_n obtained is 22.8 % of nC^* for $n = 1$. The fraction of predicted asymptotic capacity achieved in simulated channels increases as n increases. In this case, \bar{C}_n reaches 54 %, 59 % and 64 % of nC^* for $n = 4, 9, 16$ respectively. The decrease in capacity when d is small is due to the correlation between the fading gains, H_{ij} , which is not captured in the theoretical model used to derive asymptotic results, which assumes H_{ij} to be i. i. d.. As the antenna spacing is increased to 1λ and 5λ , correlation between antenna pairs is reduced and therefore \bar{C}_n more closely approaches nC^* , as shown in Fig. 6(a). For $d = 5\lambda$, the simulated channels have average capacity \bar{C}_n that reaches 70 %, 84 % and 89 % of the predicted limit nC^* for $n = 4, 9$ and 16 , respectively.

Fig. 6(b) shows an analogous comparison between \bar{MI}_n and nMI^* . As d is increased from 0.5λ to 1λ and 5λ , \bar{MI}_n increases monotonically and more closely approaches nMI^* at each value n . For $n = 4, 9, 16$, \bar{MI}_n also reaches 70 %, 84 % and 89 % of nMI^* , respectively.

In the limit of large n , C_n/n and MI_n/n converge almost surely to C^* and MI^* according to our asymptotic results. We try to study this asymptotic behavior of the capacities computed using WiSE simulated channels in the case when ρ is large. The empirical probability density functions (PDFs) of C_n/n are plotted for $n = 4, 9$ and 16 with $d = 0.5\lambda$ in Fig. 7(a) and $d = 5\lambda$ in Fig. 7(b). As n increases, the PDF of C_n/n becomes narrower with higher peak value, i.e. C_n/n becomes less random. In the limit of large n , we expect the PDF of C_n/n to converge to an impulse function centered at the value C^* . This illustrates the almost-surely convergence of C_n/n to C^* . Note that when d is large (5λ), the PDF of C_n/n grows narrower and taller much faster than when d is small (0.5λ). This indicates that the rate of convergence is higher when d is larger, i.e. when the correlation between H_{ij} is less. Further analysis is needed to understand how correlation affects the validity of the asymptotic results in Section III-C.

V. Conclusions

There is a potentially huge gain in capacity when multiple antennas are employed for an indoor wireless transmission system compared to a single antenna system. The achievable rates, C_n and MI_n , depend on the propagation environment, and grow with the increase of average received SNR ρ , number of antennas n , and antenna separation d . With perfect channel knowledge at the transmitter, power can be allocated efficiently over different transmitting antennas to achieve better rates, C_n . The water filling gain is more significant when there are fewer strong eigenmodes (71.4 % for $n = 36$ in room L175 compared to 0.06 % in L117). The benefit of water-filling is also more obvious at low average received SNR, e.g. when $\rho = -10$ dB, water filling yields 3.5 times larger capacity at 5 % outage probability ($C_n^{0.05}/MI_n^{0.05} = 3.5$), but at $\rho = 50$ dB, water filling gain is negligible ($C_n^{0.05}/MI_n^{0.05} \approx 1$).

Assuming i. i. d. channels between different antenna pairs, theoretical analysis shows that the capacity grows linearly asymptotically with the number of antennas n , in the limit of large n . However, in a more realistic propagation environment, correlation does exist between antenna pairs and causes a smaller rate of growth in capacity when n grows large. Our simulation results show that for 0.5λ antenna spacing, the simulated average capacity \bar{C}_n is only 64 % of the predicted value nC^* for $n = 16$. When the antenna spacing is increased, we see more agreement between \bar{C}_n and nC^* . Indeed

with $d = 5 \lambda$, the \bar{C}_n achieved at $\rho = 40$ dB is 89 % of nC^* when $n = 16$. To utilize MEA systems in the most efficient way, we need to choose appropriate antenna spacing d , transmit power P_{tot} , and decide on the best arrangement of antenna elements in an array as well as the actual locations of transmitting and receiving MEAs.

VI. Acknowledgments

I would like to express my sincere appreciation to Professor Joseph Kahn and Professor David Tse for their guidance and encouragement during this work. The opportunity of working closely with them have been a stimulating and rewarding experience in my Master program.

I am grateful to Reinaldo Valenzuela, Jerry Foschini, Jonathan Ling and Dmitry Chizhik for allowing us to use their WiSE simulation tools, and for their valuable advice & suggestions. Discussion with Jack Salz is equally enlightening. In addition, I truly appreciate my EE comrade, Da-Shan Shiu for patiently sharing with me his broad range of knowledge. His strong faith in me is a valuable source of motivation. The many heated discussions and arguments we had certainly help sharpen my critical thinking. I am also thankful to Ma Yi who has tutored me in EE226 during my first semester at Berkeley. Surviving the course keeps me in graduate school, and it also helps to build the background knowledge that I need for further research work.

Special thanks are dedicated to Professor David Goodman, Professor Roy Yates and Professor Christopher Rose at Rutgers University, who have motivated me to come to graduate school. Their advice will guide me a long way in life, both in college and after graduation.

I am extremely fortunate to be surrounded by friends who are caring and understanding. They have become my extended family at Berkeley. I want to take this opportunity to thank my soul mates, Ching Shang and Fang-Pei Chen, for always being there for me. I cherish every moment of their company. I would like to thank Jocelyn Nee and Janice Hudgings in particular for their emotional support, to Gene Cheung, Then Then Tan, Kean Hock Yeap, Niny Khor, Amy Aweisbin and Tz-Yin Lin for their encouragement. I also wish to thank David Lee for helping me with all sorts of computer problems and thank all the group members for sharing their expertise and humor all these past years.

I wish to thank the U.C. Berkeley EECS department, Tau Beta Pi and Schumberger Cooperation, whose financial support made my graduate program possible.

Last but not least, I won't have accomplished this without the love and support of my family members, who are far away in distance but close at heart. They are always available with love and patience, through all my past twenty four years. In my heart, my family is the greatest masterpiece on earth.

VII. References

- [1] W. Jakes Jr., *Microwave Mobile Communications*, New Wiley, 1974.
- [2] J. Winters, "Optimum Combining for Indoor Radio Systems with Multiple Users", *IEEE Trans. Commun.*, vol. com-35, no. 11, pp. 1222-1230, Nov. 1987.
- [3] G. J. Foschini and M. J. Gans, "On Limits of Wireless Communication in a Fading Environment When Using Multiple Antennas", accepted for publication in *Wireless Personal Communications*.
- [4] G. J. Foschini and M. J. Gans, "Capacity When Using Diversity At Transmit And Receive Sites and The Rayleigh-Faded Matrix Channel Is Unknown At The Transmitter", *WINLAB Workshop on Wireless Information Network*, March 20-21, New Brunswick, NJ.
- [5] S. J. Fortune, D. H. Gay, B. W. Kernighan, O. Landron, R. A. Valenzuela and M. H. Wright, "WiSE design of Indoor Wireless Systems: Practical Computation and Optimization", *IEEE Computational Science and Engineering*, Mar. 1995.
- [6] G. J. Foschini and R. A. Valenzuela, "Initial Estimation of Communication Efficiency of Indoor Wireless Channels", *Wireless Network*, vol.3, no. 2, pp. 141-54, 1997.
- [7] T. M. Cover and J. A. Thomas, *Elementary of Information Theory*, John Wiley & Sons, New York, 1991.
- [8] I. E. Telatar, "Capacity of Multi-antenna Gaussian Channels", AT&T Bell Laboratories, Murray Hill, NJ.
- [9] V.A. Marcenko, and L.A. Pastur, "Distribution of Eigenvalues for Some Sets of Random Matrices", *USSR-Sb. 1*, 457-483, 1967.
- [10] Y.Q. Yin, "Limiting Spectral Distribution for A Class of Random Matrices", *Journal of Multivariate Analysis*, 20: 50-68, 1986.
- [11] Jack Silverstein, "Strong Convergence of the Empirical Distribution of Eigenvalues of large Dimensional Random Matrices", *Journal of Multivariate Analysis*, 55(2):331-339, 1995.

VIII. Tables

number of antennas, n	1	4	9	16	25	36
$C_n^{0.05}$ (bps/Hz)	19.14	60.70	126.86	211.51	334.36	459.58
$MI_n^{0.05}$ (bps/Hz)	19.14	60.69	126.83	211.40	334.21	459.30
% difference	0.00	0.00	0.02	0.05	0.45	0.06

Table 1a: L117

number of antennas, n	1	4	9	16	25	36
$C_n^{0.05}$ (bps/Hz)	8.86	20.02	36.28	56.87	75.36	106.25
$MI_n^{0.05}$ (bps/Hz)	8.63	18.93	33.83	52.29	68.23	95.43
% difference	2.65	5.73	7.22	8.75	10.44	11.32

Table 1b: L147

number of antennas, n	1	4	9	16	25	36
$C_n^{0.05}$ (bps/Hz)	2.45	6.32	10.01	14.05	20.10	26.23
$MI_n^{0.05}$ (bps/Hz)	2.44	4.59	6.65	10.31	12.20	15.30
% difference	0.19	37.78	50.51	36.28	64.80	71.40

Table 1c: L175

Table 1: The percentage difference, $(C_n^{0.05} - MI_n^{0.05})/MI_n^{0.05} \times 100 \%$, for room (a) L117 (b) L147 and (c) L175. $\rho = 38$ dB, $d = 0.5 \lambda$.

IX. Figures

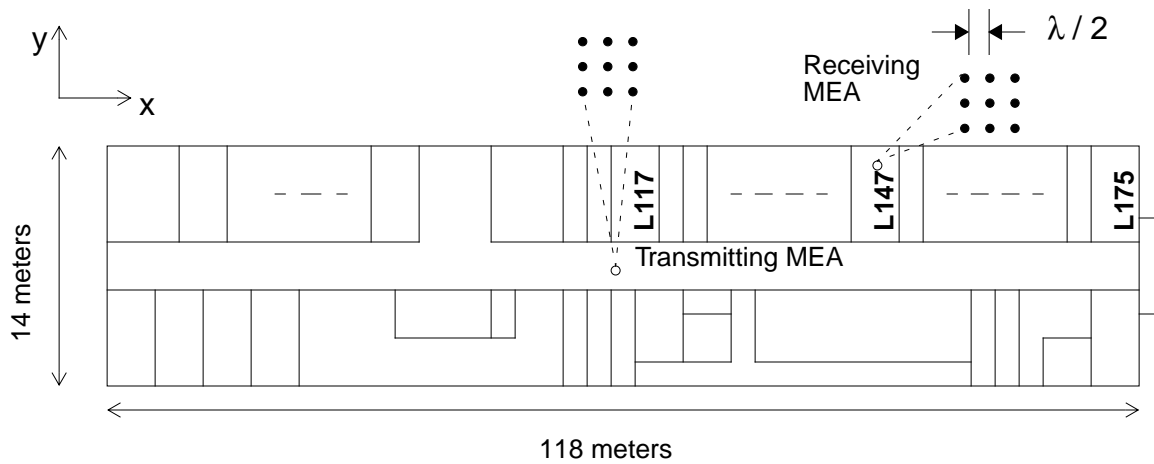


Fig. 1. Floor Plan for the first floor of Bell Laboratories Building at Crawford Hill, New Jersey. Receivers with antennas positioned in square grids are placed randomly at 1000 locations in room L117, L147 and L175. The transmitting MEA is placed with its adjacent sides parallel to x-axis and y-axis, respectively. The receiving MEA is placed with random orientation at each of the sample location.

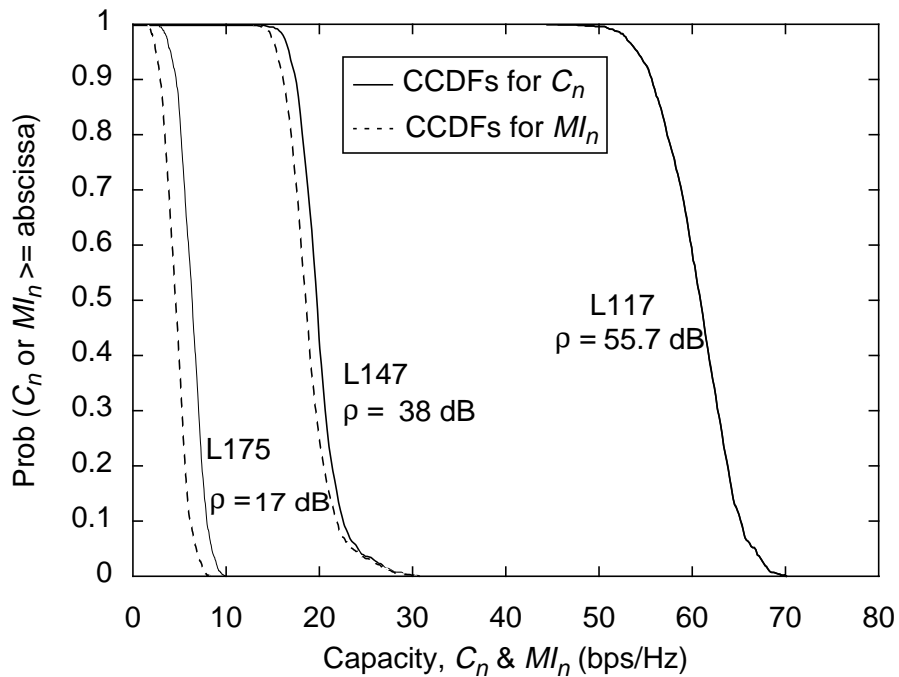


Fig. 2. The CCDFs of C_n (solid curve) and MI_n (dashed curve). C_n is the capacity with optimum water-filling power allocation, and MI_n is the mutual information with flat power allocation. P_{tot}/N_0 is fixed at 120.8 dB and the measured ρ is indicated for the three rooms.

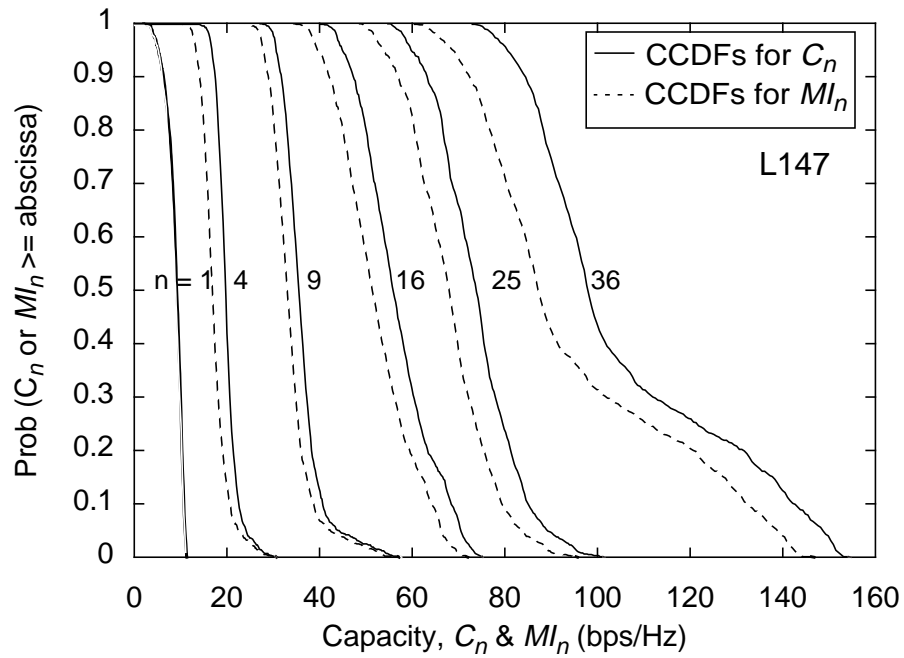


Fig. 3. The CCDFs of C_n (achieved via water pouring) and MI_n (with equal power allocation) for L147 with equal number of antennas at both transmitter and receiver ($n= 1, 4, 9, 16, 25$ & 36) at received $\rho = 20\text{dB}$.

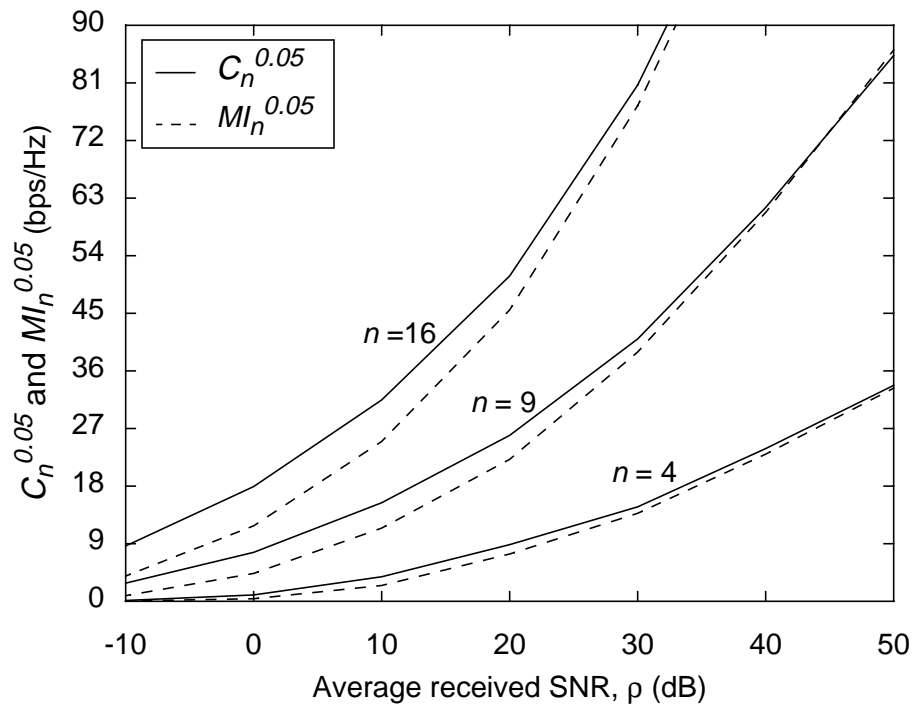


Fig. 4(a). $C_n^{0.05}$ (capacity with optimum water-filling power allocation) and $MI_n^{0.05}$ (mutual information with flat power allocation) at 5 % outage probability for receivers in room L147.

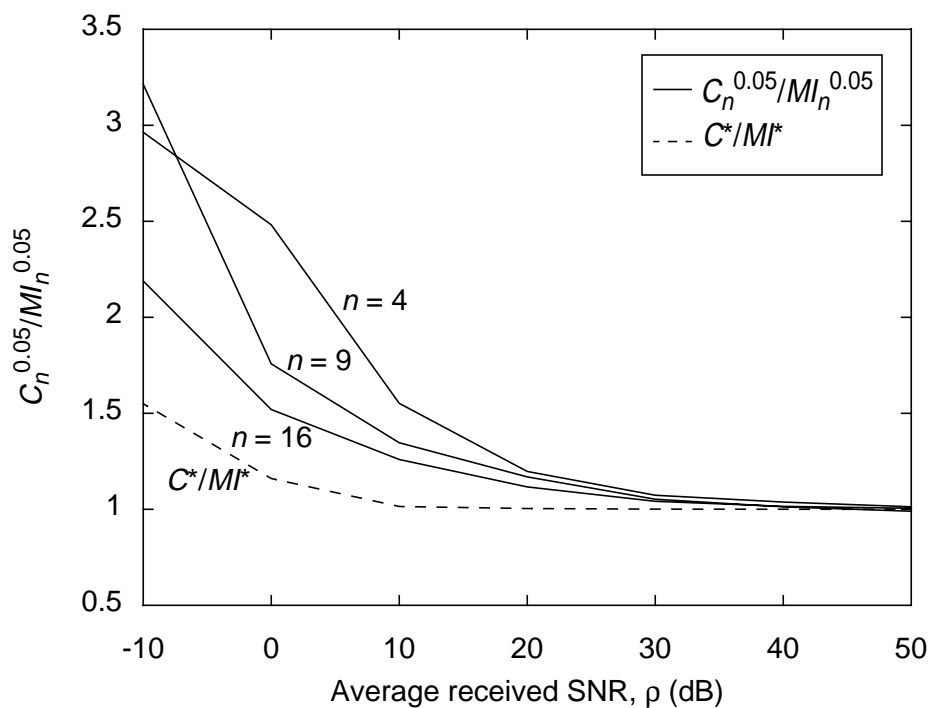


Fig. 5(a). Water-filling gain $C_n^{0.05}/M_n^{0.05}$ (solid lines) over varying average received SNR, ρ , in room L147 for $n = 4, 9$ and 16 . The reference curve is C^*/M^* (dashed line) is predicted by asymptotic theory in Section III-C.

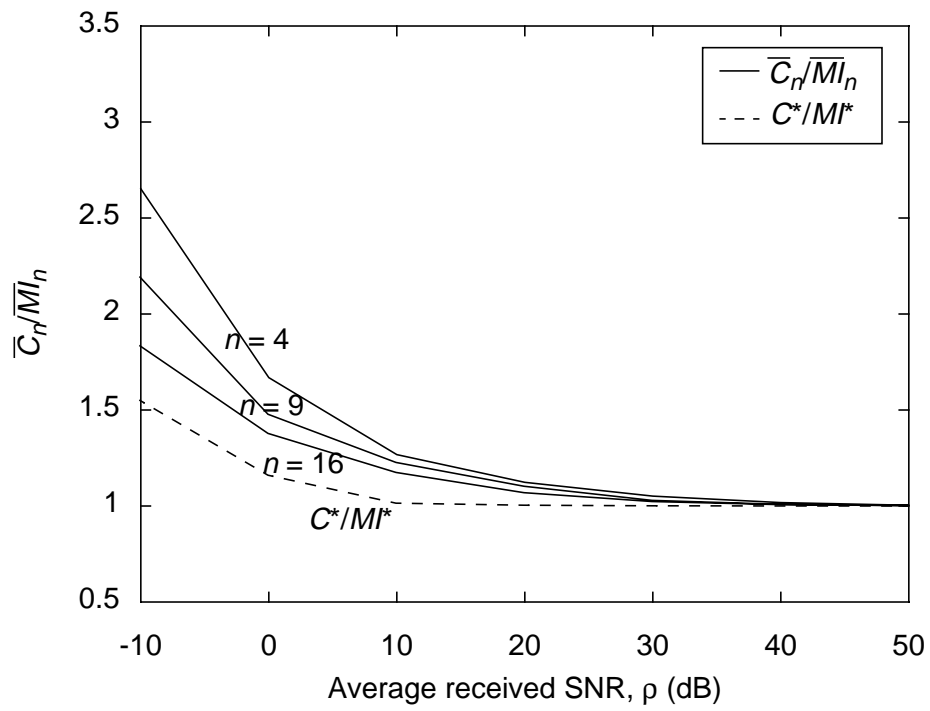


Fig. 5(b). Water-filling gain \bar{C}_n/\bar{M}_n (solid lines) over varying average received SNR, ρ in room L147 for $n = 4, 9$ and 16 . The reference curve is C^*/M^* (dashed line) is predicted by asymptotic theory in Section III-C.

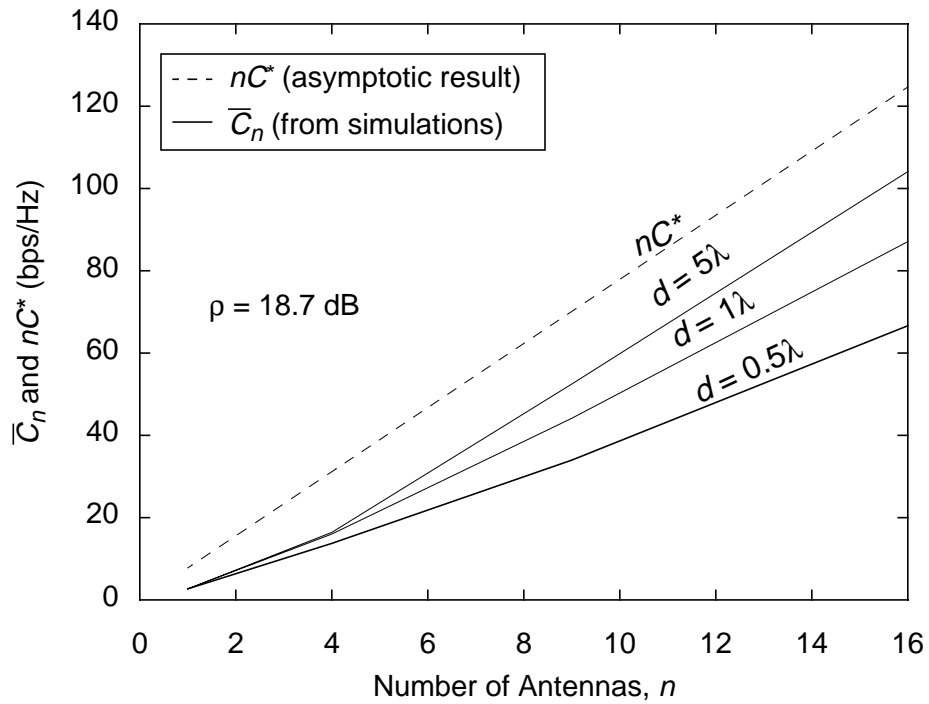


Fig. 6(a). Average \bar{C}_n with optimum water-filling power allocation in room L147 for different antenna spacing as n is increased from 1 to 16. The reference curve (dashed line) is nC^* , which is predicted by asymptotic theory using variance v^2 computed from WiSE channels.

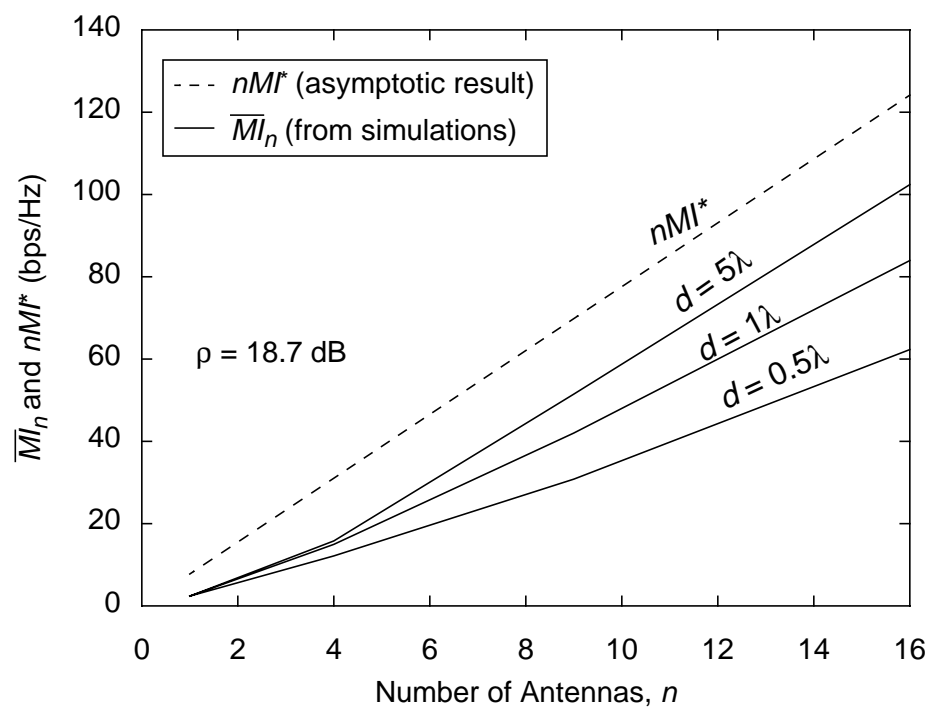


Fig. 6(b). Average \overline{MI}_n with equal power allocation in room L147 for different antenna spacing as n is increased from 1 to 16. The reference curve (dashed line) is nMI^* .

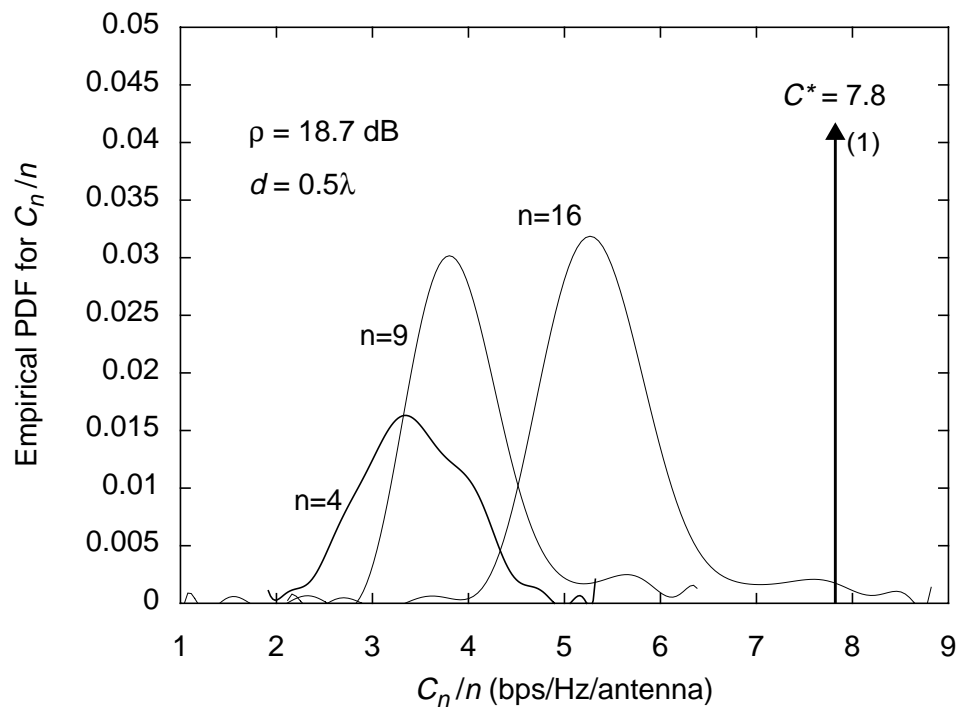


Fig. 7(a). Empirical probability density function for the normalized capacity C_n/n for $n = 4, 9$ and 16 . The reference value is C^* , the constant that C_n converges to as predicted by the asymptotic theory. Antenna spacing $d = 0.5\lambda$.

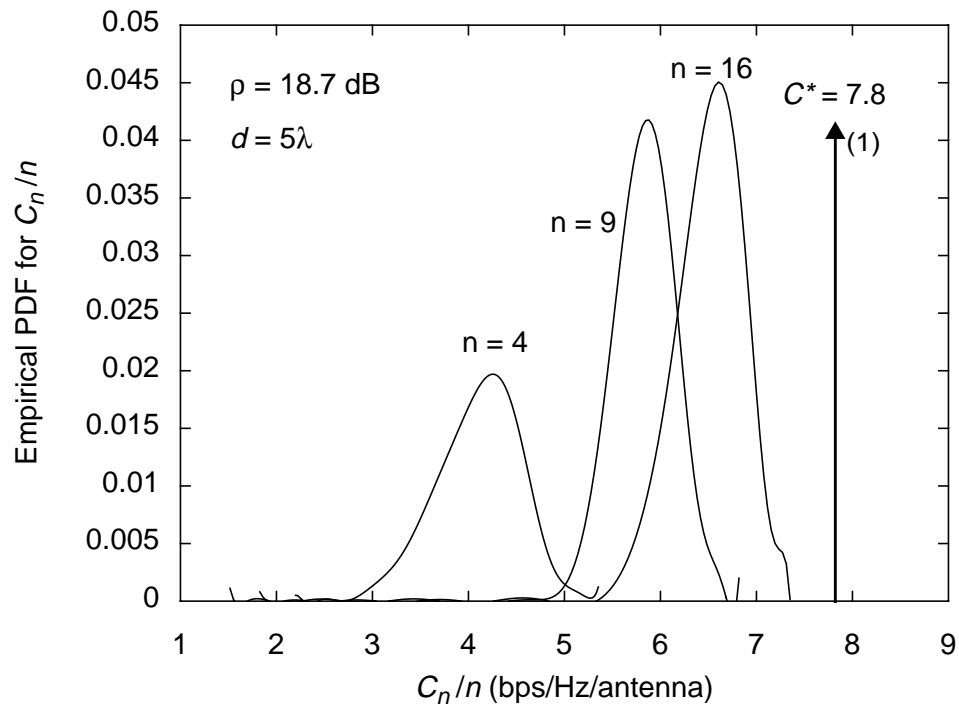


Fig. 7(b). Empirical probability density function for the normalized capacity C_n/n for $n = 4, 9$ and 16 . The reference value is C^* , the constant that C_n converges to as predicted by the asymptotic theory. Antenna spacing $d = 5\lambda$.

Appendix A: Capacity for Channels with Frequency-Selective Fading

We will extend the result to the frequency-selective fading case. Consider $H(f)$ where each entry is a function of frequency. Assume the signal is bandlimited to W Hz. We will approximate the frequency response in piecewise-constant fashion by dividing the total bandwidth into B frequency bins of width Δf , each of which is narrow enough so that $H(f)$ is approximately flat within the bin. Applying SVD separately to each frequency band $m = 1, 2, \dots, B$, we have

$$\hat{H}(m) = \hat{U}(m)\hat{D}(m)\hat{V}^\dagger(m).$$

The capacity per unit bandwidth can be approximated as:

$$\frac{C_n}{W} = \frac{C_n(H, W, P_i, P_{\text{tot}})}{B \cdot \Delta f} \approx \frac{1}{B} \cdot \sum_{m=1}^B \left\{ \sum_{i=1}^{\min\{T, R\}} \log \left(\frac{\lambda_i(m) \cdot \tilde{Q}_{ii}(m)}{N_o} + 1 \right) \right\}, \quad (20)$$

where \tilde{Q}_{ii}^* are chosen to meet the power constraints:

$$\sum_{m=1}^B \sum_{i=1}^T \tilde{Q}_{ii}^*(m) \leq P_{\text{tot}}, \quad (20a)$$

$$\sum_{m=1}^B \sum_{i=1}^T |V_{ji}(m)|^2 \cdot \tilde{Q}_{ii}^*(m) \leq P_j \quad \text{for } j = 1, 2, 3, \dots, T. \quad (20b)$$

Assuming that signals in different frequency bins are orthogonal to one another, the channel reduces to parallel Gaussian channels that provide BT degrees of freedom in choosing the variances of the T signals transmitted in B frequency sub-bands.